Table IV. Crystallographic Data for $Cp^*Cr(NO)(O\text{-}i\text{-}Pr)_2$

chem formula $C_{16}H_{29}NO_3Cr$	space group $P2_1/n$ (No. 14)
a = 9.535 (3) Å	fw 335.4
b = 9.789 (4) Å	λ = 0.71073 Å
c = 20.108 (9) Å	ρ_{calcd} = 1.188 g/cm^3
β = 91.89 (5)°	μ = 0.602 mm^{-1}
V = 1875.8 (13) Å^3	R^a = 0.0571
Z = 4	$R_w{}^b$ = 0.0649
T = 21 °C	

$^a R = \sum||F_o| - |F_c||/\sum|F_o|$. $^b R_w = [\sum w(|F_o| - |F_c|)^2/\sum w|F_o|^2]^{1/2}$; $w = 1/\sigma^2(|F_o|)$.

in CH_2Cl_2 showed no appearance of a carbonyl-containing product or disappearance of starting material.

Attempted Addition of PPh_3 or Iodide to $Cp^*Cr(NO)(O\text{-}i\text{-}Pr)_2$. A benzene solution containing an equimolar amount of PPh_3 and $Cp^*Cr(NO)(O\text{-}i\text{-}Pr)_2$ was heated at reflux for 30 min. A separate tube containing an equimolar amount of [PPN]I and $Cp^*Cr(NO)(O\text{-}i\text{-}Pr)_2$ was treated similarly. Monitoring these reactions by ^{1}H NMR and IR spectroscopy did not show the appearance of any new species or the disappearance of starting material.

Thermolysis of $Cp^*Cr(NO)(O\text{-}i\text{-}Pr)_2$. A 5-mm NMR tube containing ca. 0.01 g of $Cp^*Cr(NO)(O\text{-}i\text{-}Pr)_2$ was attached to a vacuum manifold and placed under an N_2 atmosphere. The tube was heated at 150 °C using a preheated oil bath for 1 min, and then the oil bath was replaced by a Dewar vessel containing liquid N_2. After cooling, the system was evacuated and $CDCl_3$ was vacuum transferred to the cold tube. After thawing, the tube was examined by ^{1}H NMR spectroscopy.

X-ray Structure Determination for $Cp^*Cr(NO)(O\text{-}i\text{-}Pr)_2$. Crystals suitable for X-ray analysis were grown by vacuum sublimation at 35 °C onto a water-cooled finger. A dark plate measuring 0.10 mm × 0.35 mm × 0.45 mm was selected and flame sealed inside a 0.5-mm glass X-ray capillary. The centering of 20 reflections in the range $35° < 2\theta < 10°$ lead to the selection of a primitive monoclinic cell. An axial photograph indicated symmetry along the unique (b) axis. The θ–2θ data set was collected at room temperature. The structure was solved by direct methods, and remaining non-hydrogen atoms were located by subsequent difference maps. The data solution and refinement procedures utilized the SHELXTL or SHELXTL PLUS package of programs (formerly Nicolet, presently Siemens Corp., Madison, WI). Table IV lists a summary of the crystallographic data. The small variation of ψ-scan intensity data indicated that an absorption correction was unnecessary.

Acknowledgment. The support of the National Science Foundation (Grant CHE-8901855) is gratefully acknowledged. We also gratefully acknowledge the NSF for partial funding of the X-ray diffractometers (Vermont EPSCoR, Grant R11-8601679; Utah State University, Grant CHE-9002379) and the Utah State University Research Office. We are grateful to Professor M. T. Ashby for helpful discussions about this chemistry.

Supplementary Material Available: For $Cp^*Cr(NO)(O\text{-}i\text{-}Pr)_2$, complete listings of the X-ray data collection and refinement parameters, final anisotropic thermal parameters, and H atom coordinates (4 pages); a listing of observed and calculated structure factors (13 pages). Ordering information is given on any current masthead page.

Contribution from Ames Laboratory and the Department of Chemistry, Iowa State University, Ames, Iowa 50011

Mono- and Dinuclear Complexes of a New Binucleating Porphyrin, α,α-5,15-Bis(*o*-(nicotinoylamino)phenyl)-2,8,12,18-tetraethyl-3,7,13,17-tetramethylporphyrin. Crystal Structures of a Mononuclear Nickel(II) Complex and a Binuclear Cu–Pt Complex

L. Keith Woo,* Mannar R. Maurya, Robert A. Jacobson,* Shumei Yang, and Sharon L. Ringrose

Received July 30, 1991

The synthesis and characterization of a new binucleating porphyrin ligand, α,α-5,15-bis(*o*-(nicotinoylamido)phenyl)-2,8,12,18-tetraethyl-3,7,13,17-tetramethylporphyrin, $[H_2(DPE)]\text{-}(py)_2$ is reported. Treatment of $[H_2(DPE)]\text{-}(py)_2$ with methanol solutions of Ni(II) or Cu(II) leads to the formation of mononuclear metal complexes, $[M(DPE)]\text{-}(py)_2$, in which the metal has inserted into the porphyrin core, leaving the pyridine binding site free. Addition of a second metal to form a binuclear complex, $[M(DPE)]\text{-}(py)_2M'Cl_2$, can be accomplished using the reagent $M'(DMSO)_2Cl_2$, M' = Pd, Pt, and Zn. $[Ni(DPE)]\text{-}(py)_2$ and $[Cu(DPE)]\text{-}(py)_2PtCl_2$ have been characterized by single-crystal X-ray analysis. Crystal data for $[Ni(DPE)]\text{-}(py)_2$: $NiO_2N_8C_{56}H_{52}\cdot 2CHCl_3$, triclinic, $P\bar{1}$, a = 14.306 (4) Å, b = 14.719 (5) Å, c = 14.296 (5) Å, α = 94.86 (3)°, β = 96.38 (3)°, γ = 63.45 (2)°, Z = 2, R = 0.049, and R_w = 0.064. Crystal data for $[Cu(DPE)]\text{-}(py)_2PtCl_2$: $CuPtO_2N_8C_{56}H_{52}$, triclinic, $P\bar{1}$, a = 19.333 (1) Å, b = 23.74 (1) Å, c = 12.984 (5) Å, α = 103.28 (4)°, β = 108.29 (3)°, γ = 76.47 (3)°, Z = 4, R = 0.073, and R_w = 0.085. Pt–Pt distances between the two molecules in the asymmetric unit are 3.766 (3) Å.

Multinuclear transition-metal complexes have been intensely studied as active-site models[1] of enzymes whose functions are believed to require the presence of more than one metal. Additional interest in multimetallic systems derives from the possibility of developing special chemical and physical properties as a result of the mutual interaction of two or more metal centers.[2] The potential for developing new catalysts or catalytic reactions also provides a strong driving force for continuing research in this field.[3] Particularly intriguing is the possibility of discovering new processes which cannot be mediated by the individual metal components alone.

Preparation of discrete multinuclear complexes relies heavily on ligand design. For binuclear metal systems, important ligand features include the presence of two distinct, well-defined binding sites which position the metals in close proximity. The ability to vary the identity of the two metals and the metal–metal separation is also a desirable attribute. For these reasons, we have utilized porphyrins as the basis of our binucleating ligand systems. The porphyrin ligand can bind a wide range of metals and is easily

(1) Que, L., Jr., Ed. *Metal Complexes in Proteins*; American Chemical Society: Washington, DC, 1988.
(2) Interrante, L. V., Ed. *Extended Interactions between Metal Ions*; ACS Symposium Series; American Chemical Society: Washington, DC, 1974.
(3) (a) Collman, J. P.; Rothrock, R. K.; Finke, R. G.; Moore, E. J.; Rose-Munch, F. *Inorg. Chem.* **1982**, *21*, 146. (b) Casey, C. P.; Bullock, R. M.; Fultz, W. C.; Rheingold, A. L. *Organometallics* **1982**, *1*, 1591. (c) Casey, C. P.; Nief, F. *Organometallics* **1985**, *4*, 1218.

0020-1669/92/1331-0913$03.00/0

functionalized with additional chelating appendages.

We have recently begun an investigation of multinuclear transition-metal complexes derived from difunctionalized porphyrin ligands.[4,5] The framework of our multichelating ligand is based on α,α-bis(*o*-aminophenyl)-2,8,12,18-tetraethyl-3,7,13,17-tetramethylporphyrin, H_2(DPE) (*di*[*o*-aminophenyl]*etio*porphyrin), which was originally prepared by Chang.[6] We recently reported the synthesis of the α,α-bis(β-alanyl) appended H_2(DPE) and structurally characterized a mononuclear complex of this multifunctional ligand.[4] We have subsequently shown that a variety of trinuclear complexes can be prepared with this multichelating ligand.[5]

As an extension of our work on multinuclear metal systems, we have functionalized H_2(DPE) with a bis(pyridine) binding site. We report herein the synthesis of this new ligand and the preparation of a variety of novel binuclear metal complexes. Single-crystal X-ray structure analyses are also reported for a mononuclear nickel complex and a binuclear Cu–Pt complex.

Experimental Section

Commercial reagents were used as received unless otherwise noted. THF was freshly distilled from purple solutions of Na/benzophenone under nitrogen. α,α-5,15-bis(*o*-aminophenyl)-2,8,12,18-tetraethyl-3,7,13,17-tetramethylporphyrin, H_2(DPE), was synthesized according to the method reported elsewhere.[6] *cis*-Pt(DMSO)$_2$Cl$_2$, *trans*-Pd(DMSO)$_2$Cl$_2$,[7] and Zn(DMSO)$_2$Cl$_2$[8] were prepared by following the literature procedures. Elemental analysis was performed by Oneida Research Services, Inc., Oneida, NY. ^{1}H NMR spectra were recorded on a Nicolet NIC 300-MHz or Varian VXR 500-MHz spectrometer using CD_2Cl_2 or $CDCl_3$ as solvent. FAB mass spectra were obtained on a Kratos MS-50 spectrometer. Visible spectra were recorded on a HP 8452A diode-array spectrophotometer using CH_2Cl_2 as solvent. IR spectra were run on an IBM IR-98 Fourier transform infrared spectrophotometer.

α,α-5,15-Bis(*o*-(nicotinoylamino)phenyl)-2,8,12,18-tetraethyl-3,7,13,17-tetramethylporphyrin, [H_2(DPE)]-(py)$_2$ (1). Triethylamine (6.6 mL) and nicotinoyl chloride hydrochloride (1.78 g, 10 mmol) were stirred in 450 mL of THF under nitrogen for 3 h. A solution of H_2(DPE) (0.66 g, 1 mmol) in THF (250 mL) was added under nitrogen, and the reaction mixture was heated at reflux for 15 h anaerobically. CH_3COONa (8 g) was added, and heating was continued for 10 h. After cooling of the reaction mixture to ambient temperature, it was filtered and the residues were washed with THF. The combined THF fractions were evaporated to dryness, the resulting solid was redissolved in 400 mL of CH_2Cl_2, and the solution was washed successively with water (500 mL), saturated $NaHCO_3$ (500 mL), and water (2 × 500 mL), dried over $MgSO_4$, filtered, and concentrated to 10 mL. After addition of 300 mL of hexanes, the solution was cooled to −10 °C overnight. A purple crystalline solid was filtered out, washed with hexanes, and dried under reduced pressure at ambient temperature. Yield: 0.66 g, 76%. Anal. Calcd for $C_{56}H_{54}N_8O_2\cdot H_2O$: C, 75.68; H, 6.31; N, 12.61. Found: C, 75.64; H, 6.27; N, 12.51. UV–vis (CH_2Cl_2): 410 (Soret), 508, 542, 576, and 626 nm. FABMS (MH$^+$): found, *m/e* 871.4; calcd, *m/e* 871.2. ^{1}H NMR (500 MHz, $CDCl_3$): δ 10.29 (s, 2 H, *meso*-H), 9.00 (dd, J = 8.0 Hz, J = 1.0 Hz, 2 H, H_3 aryl), 8.00 (dd, J = 5.0 Hz, J = 1.5 Hz, 2 H, H_6 py), 7.98 (d, J = 1.8 Hz, 2 H, H_2 py), 7.95 (s, 2 H, NHCO), 7.93 (td, J = 8.0 Hz, J = 8.0 Hz, J = 1.5 Hz, 2 H, H_4 aryl), 7.88 (dd, J = 7.5 Hz, J = 1.5 Hz, 2 H, H_6 aryl), 7.60 (td, J = 8.0 Hz, J = 7.5 Hz, J = 1.0 Hz, 2 H, H_5 aryl), 6.79 (dt, J = 8.0 Hz, J = 2 Hz, J = 1.5 Hz, 2 H, H_4 py), 6.40 (dd, J = 8.0 Hz, J = 1.8 Hz, 2 H, H_5 py), 4.03 (q, 8 H, CH_2CH_3), 2.60 (s, 12 H, CH_3), 1.77 (t, 12 H, CH_2CH_3), 1.51 (s, 2 H, H_2O), −2.34 (s, 2 H, NH pyrrole).

[Ni(DPE)]-(py)$_2$ (2). Nickel acetate (0.072 g, 0.29 mmol) in 10 mL of MeOH was added to a solution of [H_2(DPE)]-(py)$_2$ (0.25 g, 0.28 mmol) in 50 mL of $CHCl_3$/MeOH (9:1). After heating of the reaction mixture at reflux for 10 h, the solvent was removed under reduced pressure. The residues were suspended in 250 mL of water containing 1 M HCl (8 mL) and stirred for 2 h. The suspension was extracted with CH_2Cl_2 (2 × 100 mL), washed with water, dried over $MgSO_4$, filtered, and concentrated to 5 mL. This solution was layered with 25 mL of hexanes and cooled to −10 °C for 4 h. The precipitate was filtered out, washed with hexanes, and dried in vacuo at ambient temperature to yield 0.225 g (84%) of red solid. Anal. Calcd for $C_{56}H_{52}N_8O_2Ni\cdot H_2O$: C, 71.13; H, 5.72; N, 11.86. Found: C, 71.52; H, 5.79; N, 11.88. UV–vis (CH_2Cl_2): 408 (Soret), 530, and 566 nm. FABMS (MH$^+$): found, *m/e* 927.1; calcd, *m/e* 927.69. ^{1}H NMR (CD_2Cl_2): δ 9.54 (s, 2 H, meso), 8.88 (d, 2 H, H_3 aryl), 8.16 (m, 2 H, H_6 py), 8.09 (s, 2 H, NH), 7.96 (d, 2 H, H_2 py), 7.83 (m, 2 H, aryl), 7.48 (m, 4 H, aryl), 6.85 (m, 2 H, H_4 py), 6.57 (m, 2 H, H_5 py), 3.74 (m, 8 H, CH_2CH_3), 2.34 (s, 12 H, CH_3), 1.55 (t, 12 H, CH_2CH_3). IR (mull): ν_{CO} = 1684 (m) cm^{-1}.

[Cu(DPE)]-(py)$_2$ (3). This complex was prepared using the method described above with copper acetate (0.058 g, 0.29 mmol) and [H_2-(DPE)]-(py)$_2$ (0.25 g, 0.28 mmol). Yield: 0.23 g, 85.9%. UV–vis (CH_2Cl_2): 410 (Soret), 534, and 570 nm. FABMS (MH$^+$): found, *m/e* 932.34; calcd, *m/e* 932.54. IR (mull): ν_{CO} = 1682 (s) cm^{-1}.

[Ni(DPE)]-(py)$_2$PtCl$_2$ (4). [Ni(DPE)]-(py)$_2$ (0.10 g, 0.11 mmol), *cis*-Pt(DMSO)$_2$Cl$_2$ (0.050 g, 0.12 mmol), and $CHCl_3$ (15 mL) were heated at reflux for 24 h. After the solvent volume was reduced to 5 mL, the reaction flask was cooled to −10 °C overnight. The pink solid was filtered out, washed thoroughly with $CHCl_3$ and CH_3OH, and dried. The compound was recrystallized from CH_2Cl_2/CH_3OH and dried under vacuo at 80 °C. Yield: 0.070 g, 56%. Anal. Calcd for $C_{56}H_{52}N_8O_2Cl_2NiPt$: C, 56.33; H, 4.36; N, 9.38. Found: C, 56.39; H, 4.33; N, 9.23. UV–vis (CH_2Cl_2): 408 (Soret), 530, and 564 nm. FABMS (MH$^+$): found, *m/e* 1193.73; calcd, *m/e* 1193.77. ^{1}H NMR (CD_2Cl_2): δ 9.43 (s, 2 H, meso), 8.79 (d, 2 H, H_3 aryl), 8.28 (dd, 2 H, H_5' py), 8.13 (dd, 2 H, H_6 aryl), 8.09 (dt, 2 H, H_4' py), 7.86 (td, 2 H, H_4 aryl), 7.63 (t, 2 H, H_5 aryl), 7.10 (d, 2 H, H_2' py), 7.09 (s, 2 H, NH), 6.85 (t, 2 H, H_6' py), 3.71 (m, 4 H, CH_2CH_3), 3.60 (m, 4 H, CH_2CH_3), 2.28 (s, 12 H, CH_3), 1.54 (t, 12 H, CH_2CH_3). IR (CH_2Cl_2): ν_{CO} = 1693 (s) cm^{-1}. Far-IR (CH_2Cl_2): ν_{Pt-Cl} = 343 cm^{-1}.

[Cu(DPE)]-(py)$_2$PtCl$_2$ (5). Using a procedure similar to that described above with [Cu(DPE)]-(py)$_2$ (0.10 g, 0.11 mmol) and *cis*-Pt(DMSO)$_2$Cl$_2$ (0.05 g, 0.12 mmol) produced 0.060 g (47%) of [Cu(DPE)]-(py)$_2$PtCl$_2$ after recrystallization from CH_2Cl_2/CH_3OH. Anal. Calcd for $C_{56}H_{52}N_8O_2Cl_2CuPt$: C, 56.11; H, 4.35; N, 9.35. Found: C, 55.85; H, 4.36; N, 9.26. UV–vis (CH_2Cl_2): 412 (Soret), 536, 572 nm. IR (CH_2Cl_2): ν_{CO} = 1678 (s) cm^{-1}. Far-IR (CH_2Cl_2): ν_{Pt-Cl} = 347 cm^{-1}.

[Ni(DPE)]-(py)$_2$PdCl$_2$ (6). This complex was prepared as described above by using [Ni(DPE)]-(py)$_2$ (0.10 g, 0.11 mmol) and *trans*-Pd(DMSO)$_2$Cl$_2$ (0.040 g, 0.12 mmol). The complex started to precipitate while the mixture was heated. After cooling of the reaction mixture to 10 °C for 4 h, the solid was filtered out and washed with chloroform and CH_3OH. Crystallization from CH_2Cl_2/CH_3OH gave a pink solid, which was dried under vacuo at 80 °C. Yield: 0.10 g, 80%. Anal. Calcd for $C_{56}H_{52}N_8O_2Cl_2NiPd$: C, 60.86; H, 4.70; N, 10.14. Found: C, 60.64; H, 4.72; N, 10.09. UV–vis (CH_2Cl_2): 408 (Soret), 530, and 266 nm. FABMS (MH$^+$): found, *m/e* 1104.57; calcd, *m/e* 1104.09. ^{1}H NMR (CD_2Cl_2): δ 9.46 (s, 2 H, meso), 8.79 (d, 2 H, H_3 aryl), 8.29 (dd, 2 H, H_6' py), 8.11 (dd, 2 H, H_6 aryl), 8.09 (dt, 2 H, H_4' py), 7.86 (td, 2 H, H_4 aryl), 7.64 (td, 2 H, H_5 aryl), 7.08 (s, 2 H, NH), 7.01 (dd, 2 H, H_5' py), 6.85 (d, 2 H, H_2' py), 3.71 (m, 4 H, CH_2CH_3), 3.62 (m, 4 H, CH_2CH_3), 2.28 (s, 12 H, CH_3), 1.55 (t, 12 H, CH_2CH_3). IR (CH_2Cl_2): ν_{CO} = 1672 (s) cm^{-1}. Far-IR (CH_2Cl_2): ν_{Pd-Cl} = 358 cm^{-1}.

[Ni(DPE)]-(py)$_2$ZnCl$_2$ (7). Zn(DMSO)$_2$Cl$_2$ (0.047 g, 0.16 mmol) and [Ni(DPE)]-(py)$_2$ (0.10 g, 0.11 mmol) in 15 mL of $CHCl_3$ were heated at reflux for 12 h. After the solution was concentrated to 5 mL, the reaction flask was cooled to 10 °C for 4 h. The precipitate was filtered out, washed with $CHCl_3$ and CH_3OH, and dried in vacuo at 80 °C. Yield: 0.093 g, 80%. Anal. Calcd for $C_{56}H_{52}N_8O_2Cl_2NiZn\cdot H_2O$: C, 62.16; H, 4.99; N, 10.36. Found: C, 62.20; H, 5.12; N, 10.26. UV–vis (DMSO): 412 (Soret), 532, 568 nm. ^{1}H NMR (DMSO-d_6): δ 9.48 (s, 2 H, meso), 9.16 (s, 2 H, NH), 8.18 (d, 4 H), 7.85 (m, 4 H, aryl), 7.64 (m, 4 H, aryl), 6.93 (d, 2 H, H_4' py), 6.73 (m, 2 H, H_5' py), 3.66 (m, 4 H, CH_2CH_3), 3.53 (m, 4 H, CH_2CH_3), 2.22 (s, 12 H, CH_3), 1.42 (t, 12 H, CH_2CH_3).

X-ray Crystal Structure Determinations. [Ni(DPE)]-(py)$_2$·2CHCl$_3$. A purple crystal of [Ni(DPE)]-(py)$_2$·2$CHCl_3$ suitable for X-ray crystal structure determination was grown by slow evaporation of a $CHCl_3$/hexanes (3:2) solution of [Ni(DPE)]-(py)$_2$ at −10 °C. A single crystal having approximate dimension of 0.40 × 0.40 × 0.35 mm was mounted on a glass fiber using epoxy and attached to a standard goniometer head. The data were collected at −60 ± 1 °C on a Rigaku AFC6R diffractometer with graphite-monochromated Mo Kα radiation (λ = 0.71069 Å) and a 12-kW rotating anode generator. The ω–2θ scan technique was used to collect the intensity data for reflections with $2\theta < 55.1°$. On the basis of packing considerations, a statistical analysis of intensity distribution, and the successful solution and refinement of the structure, the space group was found to be $P\bar{1}$. A total of 12582 reflections were collected, and 7581 unique "observed" reflections having $I > 3\sigma(I)$ were

(4) Woo, L. K.; Maurya, M. R.; Tolppi, C. J.; Jacobson, R. A.; Yang, S.; Rose, E. *Inorg. Chim. Acta* **1991**, *182*, 41.
(5) Woo, L. K.; Maurya, M. R. *Inorg. Chem.* **1991**, *30*, 4671.
(6) Young, R.; Chang, C. K. *J. Am. Chem. Soc.* **1985**, *107*, 898.
(7) Price, J. H.; Williamson, A. N.; Schramm, R. F.; Wayland, B. B. *Inorg. Chem.* **1972**, *11*, 1280.
(8) Cotton, F. A.; Francis, R. *J. Am. Chem. Soc.* **1960**, *82*, 2986.

Table I. Crystallographic Parameters for [Ni(DPE)]-$(py)_2$ and [Cu(DPE)]-$(py)_2PtCl_2$

empirical formula	$NiO_2N_8C_{58}H_{54}Cl_6$	$PtCuCl_2N_8O_2C_{56}H_{52}$
fw	1071.61	1198.62
cryst system	triclinic	triclinic
a, Å	14.306 (4)	19.333 (8)
b, Å	14.719 (5)	23.74 (1)
c, Å	14.296 (5)	12.984 (5)
α, deg	94.86 (3)	103.28 (4)
β, deg	96.38 (3)	108.29 (3)
γ, deg	63.45 (2)	76.47 (3)
V, Å^3	2674	5422 (4)
Z	2	4
space group	$P\bar{1}$ (No. 2)	$P\bar{1}$ (No. 2)
D_{calc}, g/cm^3	1.331	1.468
F_{000}	1116	2404
$\mu_{Mo K\alpha}$, cm^{-1}	6.12	31.42
radiation (λ, Å)	Mo Kα (0.71069)	Mo Kα (0.71069)
temp, °C	−60	23
no. of reflcns measd	total, 12582; unique, 12091	total, 19697; unique, 19072
corr	Lorentz–polarization, abs (transm factors 0.95–1.00)	Lorentz–polarization
no. of observns ($I > 3.00\sigma(I)$)	7581	4114
no. of variables	892	719
reflcn/param ratio	8.50	5.72
R, R_w[a]	0.049, 0.064	0.073, 0.085

[a] $R = \sum||F_o| - |F_c||/\sum|F_o|$; $R_w = [\sum w(|F_o| - |F_c|)^2/\sum wF_o^2]^{1/2}$.

used in the structure determination and refinement. The intensities of the three representative reflections were monitored periodically throughout data collection, and their intensities showed good stability of the complex. An empirical absorption correction, based on azimuthal scans of several reflections, was applied, and the data were corrected for Lorentz and polarization effects. The structure was solved by direct methods.[9] All non-hydrogen atoms were refined anisotropically. Hydrogen positions were located from a difference electron density map and refined isotropically. Full-matrix least-squares refinement of positional and thermal parameters led to convergence with a final unweighted R factor of 0.049 and a weighted R factor of 0.064. Neutral-atom scattering factors were taken from Cromer and Waber.[10] Anomalous dispersion effects were included in F_c;[11] the values for f' and f'' were those of Cromer.[12] All calculations were done using the TEXSAN crystallographic software package of Molecular Structure Corp.[13] Table I summarizes the data collection details for [Ni(DPE)]-$(py)_2$.

[Cu(DPE)]-$(py)_2PtCl_2$. Purple platelets of [Cu(DPE)]-$(py)_2PtCl_2$ were grown by slow evaporation of a $CHCl_3$/octane solution at ambient temperature. Most of the crystals were poorly diffracting, and several were tried before finally selecting the best crystal. This crystal having approximate dimensions of 0.24 × 0.03 × 0.44 mm was mounted on a glass fiber. The data were collected at 23 °C on the diffractometer described above with Mo Kα radiation (λ = 0.71069 Å) and a ω–2θ scan technique to a maximum 2θ value of 50.1°, yielding 19697 measured reflections. On the basis of packing considerations, a statistical analysis of intensity distribution, and the successful solution and refinement of the structure, the space group was determined to be $P\bar{1}$. The intensities of three representative reflections which were measured after every 150 reflections remained constant throughout data collection indicating crystal and electronic stability (no decay correction was applied). The linear absorption coefficient for Mo Kα is 31.4 cm^{-1}. Azimuthal scans of several reflections indicated no need for an absorption correction.

The structure determination was made difficult by the presence of two molecules in the asymmetric unit. Platinum, copper, and chlorine positions were determined from a Patterson superposition using a platinum–platinum vector. Least-squares refinement was then performed using the positions of platinum, copper, and chlorine atoms and the highest 129 symmetry-unique peaks from the superposition. The remaining non-hydrogen atom positions were determined from successive structure factor and electron density map calculations.

Hydrogen atom positions were calculated. The heavier atoms were refined anisotropically, and most of the lighter atoms were refined isotropically. The final cycle of full-matrix least-squares refinement[14] was based on 4114 observed reflections ($I > 3.00\sigma(I)$) and 719 variable parameters and converged with unweighted and weighted agreement factors of $R = 0.073$ and $R_w = 0.085$. Twenty-eight reflections under 5° in 2θ were deleted due to beam-stop shadow effects. Plots of $\sum w(|F_o| - |F_c|)^2$ versus $|F_o|$, reflection order in data collection, $(\sin\theta)/\lambda$, and various classes of indices showed no unusual trends. All calculations were performed using the CHES[15] crystallographic software package. Details for the data collection for [Cu(DPE)]-$(py)_2PtCl_2$ are given in Table I.

Scheme I

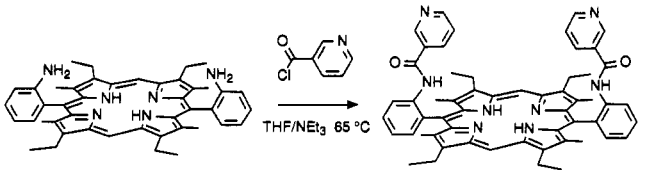

Results and Discussion

Ligand Synthesis. The condensation of H_2(DPE) with nicotinoyl chloride hydrochloride in the presence of triethylamine and anhydrous sodium acetate in THF leads to the formation of a new binucleating porphyrin, [H_2(DPE)]-$(py)_2$ (**1**), in 76% yield, as illustrated in Scheme I. No thermal atropisomerization of the aminophenyl groups occurred during the coupling reaction even though our procedure involves heating the reaction mixture in refluxing THF for several hours. The purity of the crystallized product was established by TLC, ^{1}H NMR spectroscopy, and elemental analysis. The ^{1}H NMR spectrum of **1** readily demonstrates the presence of nicotinoyl groups attached to the *o*-aminophenyl substituents of H_2(DPE). The 2-, 4-, 5-, and 6-pyridine proton signals appear at 7.98 (d), 6.79 (dt), 6.40 (dd), and 8.00 (dd) ppm, respectively. These resonances are shifted upfield relative to those of *N*-*p*-tolylnicotinamide,[16] indicating that in solution the pyridine rings spend a significant amount of time in the shielding region of porphyrin ring current.

Mononuclear Complexes. Metalation of the porphyrin core of **1** with Ni(II) and Cu(II) was achieved by treating [H_2(DPE)]-$(py)_2$ with freshly prepared solutions of the respective metal acetate in refluxing $CHCl_3/CH_3OH$. Progress of the reaction was followed by UV–vis spectroscopy. The presence of only two Q bands at the completion of the reaction clearly indicates the insertion of metal into the porphyrin core. For example, insertion of Ni(II) into [H_2(DPE)]-$(py)_2$ produces a new Q-band region with peaks at 530 and 566 nm. In addition, the ^{1}H NMR spectrum showed loss of the resonance due to the internal pyrrole protons and an upfield shift of the meso proton resonance. No appreciable shifts of the pyridine protons resonances relative to those of the unmetalated ligand are observed, indicating that the pyridine binding site remains vacant. The mononuclearity of these complexes is corroborated by mass spectral and elemental analyses. In addition, a single-crystal X-ray study was carried out on [Ni(DPE)]-$(py)_2$ (vide infra).

Dinuclear Complexes. The mononuclear complexes described above are useful precursors for the formation of dinuclear com-

(9) Gilmore, C. J. MITHRIL-an integrated direct methods computer program. (*J. Appl. Crystallogr.* **1984**, *17*, 42–46), University of Glasgow, Scotland, 1984. Beurkens, P. T. DIRDIF: Direct Methods for Difference Structures-an automatic procedure for phase extension and refinement of difference structure factors. Technical Report 1984/1 Crystallography Laboratory, Toernooiveld, 6525 Ed Nijmegen, The Netherlands.
(10) Cromer, D. T.; Waber, J. T. *International Tables for X-ray Crystallography*; The Kynoch Press: Birmingham, England, 1974; Vol. IV, Table 2.2A.
(11) Ibers, J. A.; Hamilton, W. C. *Acta Crystallogr.* **1964**, *17*, 781.
(12) Cromer, D. T. *International Tables for X-ray Crystallography*; The Kynoch Press: Birmingham, England, 1974; Vol. IV, Table 2.3.1.
(13) TEXAN-TEXRAY Structure analysis package, Molecular Structure Corp., 1985.
(14) Least-squares procedure: function minimized was $\sum w(|F_o| - |F_c|)^2$, where $w = 4F_o^2/\sigma^2(F_o)^2$.
(15) Powell, D. R.; Jacobson, R. A. FOUR: A Generalized Crystallographic Fourier Program. U.S. DOE Report IS-4737, Iowa State University, Ames, IA, 1980.
(16) NMR data for *N*-*p*-tolylnicotinamide ($CDCl_3$, 300 MHz): δ 9.07 (s, 1 H, H_2 py), 8.75 (d, 1 H, H_6 py), 8.19 (d, 1 H, H_4 py), 7.81 (s, br, NH), 7.51 (d, 2 H, aryl), 7.42 (dd, 1 H, H_5 py), 7.17 (d, 2 H, aryl), 2.34 (s, 3 H, CH_3).

Table II. Positional Parameters and B(eq) Values for $NiO_2N_8C_{56}H_{52}\cdot 2HCCl_3$

atom	x	y	z	B(eq), Å^2	atom	x	y	z	B(eq), Å^2
Ni1	0.18432 (4)	0.07216 (4)	0.18070 (4)	1.57 (3)	C22	0.4537 (4)	−0.3295 (4)	0.2429 (4)	2.9 (3)
Cl1	0.6998 (1)	0.4610 (1)	0.3680 (1)	4.6 (1)	C23	0.5177 (5)	−0.3805 (5)	0.1606 (5)	3.8 (4)
Cl2	0.8560 (1)	0.3462 (1)	0.5129 (1)	5.4 (1)	C24	0.6080 (4)	−0.0866 (4)	0.1370 (4)	3.0 (3)
Cl3	0.6402 (1)	0.4590 (1)	0.5532 (1)	4.8 (1)	C25	0.6778 (5)	−0.0818 (7)	0.2231 (5)	5.0 (5)
Cl4	0.2563 (1)	0.1915 (1)	0.4092 (1)	4.4 (1)	C26	0.5139 (4)	0.1371 (5)	0.0756 (4)	3.0 (3)
Cl5	0.3345 (1)	0.2502 (1)	0.5874 (1)	5.9 (1)	C27	0.1459 (5)	0.4682 (4)	0.2308 (5)	3.2 (3)
Cl6	0.1580 (2)	0.3970 (1)	0.4835 (1)	8.3 (2)	C28	−0.0559 (4)	0.4678 (4)	0.2972 (4)	2.9 (3)
O1	0.5337 (3)	0.3553 (3)	0.3317 (3)	4.1 (3)	C29	−0.1452 (5)	0.5265 (5)	0.2273 (5)	3.8 (4)
O2	−0.0789 (3)	−0.2224 (3)	0.3691 (2)	3.3 (2)	C30	−0.2468 (4)	0.2325 (4)	0.1778 (5)	3.0 (3)
N1	0.2380 (3)	−0.0731 (3)	0.1810 (2)	1.7 (2)	C31	−0.2893 (5)	0.3033 (6)	0.0965 (6)	5.2 (5)
N2	0.3208 (3)	0.0622 (3)	0.1673 (2)	1.9 (2)	C32	−0.1721 (4)	0.0157 (4)	0.0784 (4)	2.7 (3)
N3	0.1323 (3)	0.2169 (3)	0.1964 (2)	1.8 (2)	C33	0.3132 (3)	0.3156 (3)	0.1209 (3)	2.2 (3)
N4	0.0457 (2)	0.0826 (2)	0.1789 (2)	1.6 (2)	C34	0.3831 (3)	0.3421 (3)	0.1793 (3)	2.2 (3)
N5	0.4205 (3)	0.2929 (3)	0.2656 (3)	2.5 (3)	C35	0.4129 (4)	0.4123 (4)	0.1517 (4)	2.8 (3)
N6	−0.0399 (3)	−0.1304 (3)	0.2741 (3)	2.4 (2)	C36	0.3732 (4)	0.4566 (4)	0.0660 (4)	3.5 (4)
N7	0.5897 (4)	0.1818 (4)	0.5678 (3)	4.0 (3)	C37	0.3041 (4)	0.4322 (5)	0.0086 (4)	3.7 (4)
N8	−0.1851 (3)	0.1245 (3)	0.4579 (3)	3.6 (3)	C38	0.2744 (4)	0.3621 (4)	0.0352 (4)	2.9 (3)
C1	0.1840 (3)	−0.1319 (3)	0.1740 (3)	1.7 (2)	C39	0.0322 (3)	−0.1681 (3)	0.1228 (3)	1.8 (2)
C2	0.2556 (3)	−0.2366 (3)	0.1989 (3)	2.0 (2)	C40	0.0470 (4)	−0.2214 (4)	0.0370 (3)	2.4 (3)
C3	0.3520 (3)	−0.2401 (3)	0.2166 (3)	2.1 (3)	C41	0.0147 (4)	−0.2967 (4)	0.0159 (4)	2.9 (3)
C4	0.3412 (3)	−0.1399 (3)	0.2018 (3)	2.1 (2)	C42	−0.0316 (4)	−0.3207 (4)	0.0828 (4)	2.8 (3)
C5	0.4233 (3)	−0.1174 (4)	0.1974 (3)	2.3 (3)	C43	−0.0494 (4)	−0.2680 (4)	0.1681 (4)	2.6 (3)
C6	0.4137 (3)	−0.0251 (3)	0.1717 (3)	2.2 (3)	C44	−0.0197 (3)	−0.1903 (3)	0.1889 (3)	1.9 (2)
C7	0.4964 (3)	−0.0075 (4)	0.1415 (3)	2.4 (3)	C45	0.4955 (4)	0.2962 (4)	0.3315 (3)	2.6 (3)
C8	0.4551 (3)	0.0907 (3)	0.1177 (3)	2.3 (3)	C46	0.5282 (3)	0.2197 (4)	0.4055 (3)	2.6 (3)
C9	0.3451 (3)	0.1367 (3)	0.1396 (3)	2.0 (2)	C47	0.5383 (4)	0.1217 (4)	0.3872 (4)	3.5 (3)
C10	0.2789 (3)	0.2404 (3)	0.1484 (3)	1.9 (2)	C48	0.5770 (5)	0.0544 (5)	0.4600 (4)	4.2 (4)
C11	0.1819 (3)	0.2771 (3)	0.1863 (3)	1.8 (2)	C49	0.6014 (5)	0.0874 (5)	0.5476 (4)	4.1 (4)
C12	0.1202 (3)	0.3798 (3)	0.2219 (3)	2.1 (3)	C50	0.5553 (4)	0.2455 (5)	0.4966 (4)	3.4 (3)
C13	0.0337 (3)	0.3805 (3)	0.2532 (3)	2.1 (3)	C51	−0.0738 (3)	−0.1448 (4)	0.3539 (3)	2.3 (3)
C14	0.0394 (3)	0.2811 (3)	0.2340 (3)	1.9 (2)	C52	−0.1052 (3)	−0.0563 (4)	0.4235 (3)	2.4 (3)
C15	−0.0432 (3)	0.2581 (3)	0.2364 (3)	2.0 (2)	C53	−0.0904 (4)	−0.0740 (4)	0.5198 (4)	3.0 (3)
C16	−0.0436 (3)	0.1685 (3)	0.1991 (3)	1.9 (2)	C54	−0.1225 (4)	0.0079 (5)	0.5838 (4)	3.5 (4)
C17	−0.1356 (3)	0.1527 (3)	0.1711 (3)	2.0 (3)	C55	−0.1690 (4)	0.1052 (5)	0.5499 (4)	3.6 (4)
C18	−0.1024 (3)	0.0575 (3)	0.1316 (3)	2.0 (2)	C56	−0.1535 (4)	0.0443 (4)	0.3972 (4)	2.9 (3)
C19	0.0114 (3)	0.0108 (3)	0.1450 (3)	1.7 (2)	C57	0.7255 (4)	0.3873 (4)	0.4669 (4)	3.7 (4)
C20	0.0771 (3)	−0.0932 (3)	0.1459 (3)	1.7 (2)	C58	0.2229 (5)	0.2699 (5)	0.5120 (4)	3.7 (4)
C21	0.2303 (4)	−0.3230 (4)	0.2105 (5)	2.9 (3)					

plexes. Treatment of [M(DPE)]-(py)$_2$ with M′(DMSO)$_2$Cl$_2$ (M = Ni(II), Cu(II); M′ = Pt(II), Pd(II)) leads to the formation of dinuclear species of the type [M(DPE)]-(py)$_2$M′Cl$_2$. Elemental analysis and FAB mass spectral data confirm this formulation. [Ni(DPE)]-(py)$_2$ZnCl$_2$·H$_2$O has also been isolated by treating [Ni(DPE)]-(py)$_2$ with Zn(DMSO)$_2$Cl$_2$ in a similar manner. Reaction 1 schematically represent the formation of these com-

$$[M(DPE)]\text{-}(py)_2 + [M'(DMSO)_2Cl_2] \rightarrow [M(DPE)]\text{-}(py)_2M'Cl_2 \quad (1)$$

M = Ni(II), Cu(II); M′ = Zn(II), Pt(II), Pd(II)

plexes. All of the bimetallic complexes are insoluble in $CHCl_3$ and CH_3OH but are soluble in CH_2Cl_2, DMF, and DMSO. The exception is [Ni(DPE)]-(py)$_2$ZnCl$_2$, which is only soluble in DMF and DMSO. ^{1}H NMR spectra of the dinuclear complexes Ni–Pt and Ni–Pd in CD_2Cl_2 show distinctive changes in their proton resonances relative to that of [Ni(DPE)]-(py)$_2$. As expected, the most notable changes involve shifts of the pyridine protons resonances. For example in the Ni–Pt complex **4**, the 4′-H, 5′-H, and 6′-H signals have shifted downfield to 8.28, 6.85, and 7.10 ppm, respectively, relative to the corresponding pyridine signals in [Ni(DPE)]-(py)$_2$. This indicates that the pyridine orientation has changed upon coordination to a metal ion. In addition, methylene protons of the ethyl groups of porphyrin core split into two doublets of multiplets while methyl protons of the same groups shift slightly upfield. The meso proton signal appears at nearly the same position.

It is clear that the pair of pyridine appendages on [M(DPE)]-(py)$_2$ can serve as a good chelate for a second metal. In order to determine the coordination geometry about the palladium and platinum ions in these binuclear complexes, far-IR solution studies were undertaken. In all cases, each complex exhibits a single M–Cl stretch in the range 340–360 cm^{-1}. The appearance of a single IR-active band indicates that complexes **4–6** have trans chlorides. In the case of [Cu(DPE)]-(py)$_2$PtCl$_2$, this has been verified by single-crystal X-ray analysis (vide infra).

Crystal Structure of [Ni(DPE)]-(py)$_2$. Pertinent crystallographic parameters are collected in Table I. The asymmetric unit contains one nickel complex and two $CHCl_3$ solvate molecules. The molecular structure is shown in Figure 1 along with the atom-numbering scheme. The final atomic parameters of nonhydrogen atoms and selected intramolecular bond distances and angles are listed in Tables II and III, respectively. All bond distances and angles of the porphyrin core of the [Ni(DPE)]-(py)$_2$ molecule agree within experimental error with that of [Ni(DPE)]-(ala)$_2$ containing β-alanyl appended arms.[4] The N–Ni–N bond angles range from 88.5 (1) to 91.9 (1)° and indicate that the environment around Ni is essentially square planar. The mean deviation from the best least-squares plane, defined by the Ni atom and its four coordinated pyrrole N atoms, is 0.11 Å. The porphyrin core is nonplanar and ruffled in a manner similar to the S_4-ruffling of the tetragonal form of Ni^{II}(OEP) with an average dihedral angle of 28.6° between the mean planes of the adjacent pyrrole rings. The average Ni–N(pyrrole) distance of 1.92 Å is in the lower limit of the range reported for the majority of nickel(II) porphyrin complexes. The meso carbon atoms are displaced alternatively above and below the mean porphyrin plane by +0.57 to −0.52 Å. The distance between N(7) and N(8) is 11.4 Å, and the orientation of the N atoms of the pyridine is outward. The same orientation has also been observed in solution (vide supra). It is important to mention here that the insertion of the nickel into the porphyrin core has not caused atropisomerization of the appended nicotinamido groups.

Crystal Structure of [Cu(DPE)]-(py)$_2$PtCl$_2$. The asymmetric unit of [Cu(DPE)]-(py)$_2$PtCl$_2$ contains two molecules. The molecular structure and atom-numbering scheme for molecule A are shown in Figure 2. Atoms in molecule B are numbered

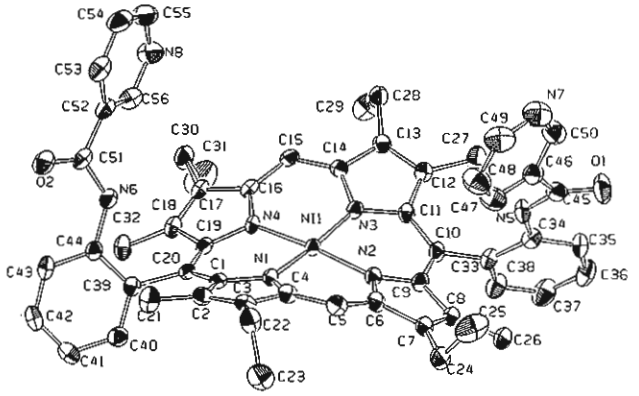

Figure 1. Molecular structure of [Ni(DPE)]-$(py)_2$ with atom-numbering scheme.

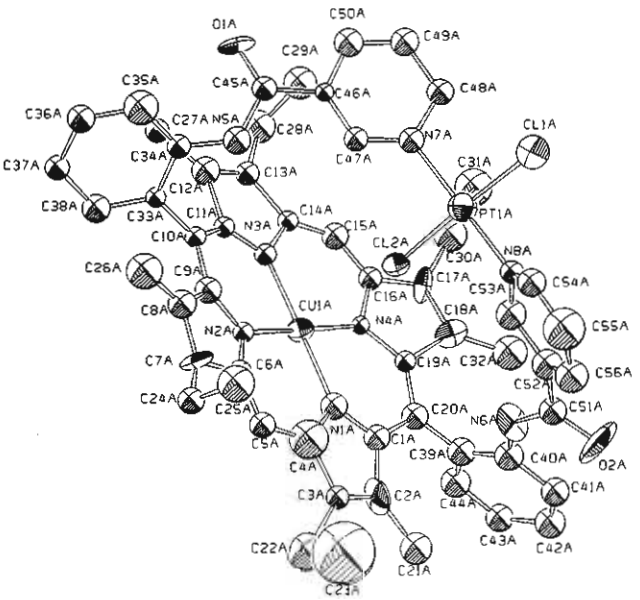

Figure 2. Molecular structure and atom-numbering scheme for molecule A of [Cu(DPE)]-$(py)_2PtCl_2$.

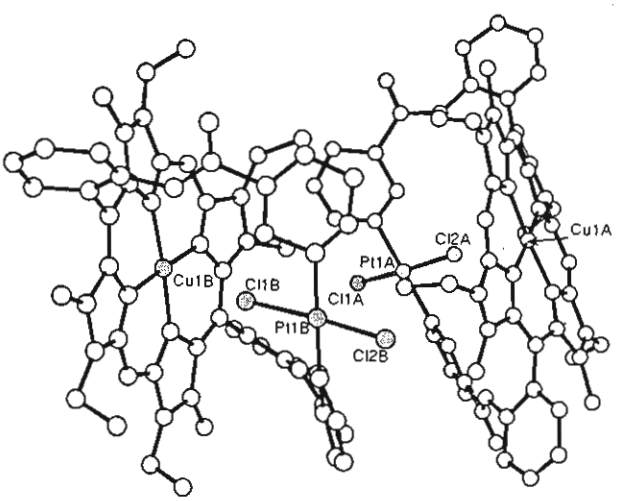

Figure 3. Asymmetric unit of [Cu(DPE)]-$(py)_2PtCl_2$.

similarly, but with the "B" designation, except Cl1 and Cl2 have been interchanged. The relationship between molecules A and B is shown in Figure 3. Table IV lists fractional coordinates for non-hydrogen atoms, and Table V gives selected bond distances and angles. The metrical parameters of the copper porphyrin fragment of this molecule are very similar to those of Cu(TPP)[17]

Table III. Selected Intramolecular Distances (Å) and Angles (deg) for [Ni(DPE)]-$(py)_2$[a]

	Distances		
	Porphyrin Skeleton		
Ni1–N1	1.922 (4)	C8–C9	1.467 (6)
Ni1–N2	1.921 (4)	C8–C26	1.494 (7)
Ni1–N3	1.919 (4)	C9–C10	1.394 (6)
Ni1–N4	1.917 (3)	C10–C11	1.399 (6)
N1–C1	1.386 (5)	C10–C33	1.492 (6)
N1–C4	1.375 (5)	C11–C12	1.449 (6)
N2–C6	1.375 (5)	C12–C13	1.358 (6)
N2–C9	1.389 (5)	C12–C27	1.495 (7)
N3–C11	1.384 (5)	C13–C14	1.433 (6)
N3–C14	1.377 (5)	C13–C28	1.503 (6)
N4–C16	1.375 (5)	C14–C15	1.372 (6)
N4–C19	1.384 (5)	C15–C16	1.382 (6)
C1–C2	1.467 (6)	C16–C17	1.445 (6)
C1–C20	1.396 (6)	C17–C18	1.355 (6)
C2–C3	1.353 (6)	C17–C30	1.504 (6)
C2–C21	1.496 (7)	C18–C19	1.453 (6)
C3–C4	1.444 (6)	C18–C32	1.500 (6)
C3–C22	1.496 (6)	C19–C20	1.393 (6)
C4–C5	1.365 (6)	C20–C39	1.502 (6)
C5–C6	1.380 (6)	C22–C23	1.503 (8)
C6–C7	1.435 (6)	C24–C25	1.514 (9)
C7–C8	1.353 (6)	C28–C29	1.501 (8)
C7–C24	1.502 (6)	C30–C31	1.512 (9)
	Nicotinoyl Groups		
O1–C45	1.215 (6)	C45–C46	1.493 (7)
O2–C51	1.216 (5)	C46–C47	1.389 (7)
N5–C34	1.411 (6)	C46–C50	1.387 (7)
N5–C45	1.363 (6)	C47–C48	1.388 (8)
N6–C44	1.418 (6)	C48–C49	1.370 (8)
N6–C51	1.356 (6)	C51–C52	1.498 (7)
N7–C49	1.333 (7)	C52–C53	1.398 (7)
N7–C50	1.340 (7)	C52–C56	1.391 (7)
N8–C55	1.343 (7)	C53–C54	1.383 (7)
N8–C56	1.336 (6)	C54–C55	1.386 (8)
	Angles		
	Porphyrin Skeleton		
N1–Ni1–N2	91.9 (1)	C1–C2–C3	106.4 (4)
N1–Ni1–N3	173.2 (1)	C1–C2–C21	128.7 (4)
N1–Ni1–N4	88.5 (1)	C3–C2–C21	124.8 (4)
N2–Ni1–N3	88.9 (1)	C2–C3–C4	107.1 (4)
N2–Ni1–N4	173.5 (2)	C2–C3–C22	128.4 (5)
N3–Ni1–N4	91.4 (1)	C4–C3–C22	124.5 (4)
Ni1–N1–C1	129.4 (3)	N1–C4–C3	111.1 (4)
Ni1–N1–C4	125.0 (3)	N1–C4–C5	124.0 (4)
C1–N1–C4	105.1 (3)	C3–C4–C5	124.4 (4)
N1–C1–C2	110.1 (4)	C4–C5–C6	124.6 (4)
N1–C1–C20	122.8 (4)	C3–C22–C23	113.5 (5)
C2–C1–C20	127.1 (4)		
	Nicotinoyl Groups		
C44–N6–C51	129.3 (4)	C51–C52–C56	123.2 (4)
C55–N8–C56	117.0 (5)	C53–C52–C56	117.4 (5)
O2–C51–N6	123.7 (5)	C52–C53–C54	119.2 (5)
O2–C51–C52	121.8 (4)	C53–C54–C55	118.6 (5)
N6–C51–C52	114.4 (4)	N8–C55–C54	123.4 (5)
C51–C52–C53	119.4 (4)	N8–C56–C52	124.3 (5)

[a] Estimated standard deviations in the least significant figure are given in parentheses.

and Cu(pincer-porphyrin).[18] The porphyrinato core is distorted from planarity to approximate S_4 symmetry. The average dihedral angle between the mean planes of adjacent pyrrole rings in molecule A is 14.4 (9)°. In addition, the meso carbons are alternately displaced above and below the mean porphyrin plane (C_5, −0.09 (3) Å; C_{10}, 0.12 (3) Å, C_{15}, −0.08 (3) Å; C_{20}, 0.04 (3) Å). The CuN_4 coordination unit also displays a slight S_4 distortion with an alternating displacement of the nitrogens above and below the mean N_4 plane by an average of 0.06 (2) Å. The porphyrin

(17) Fleischer, E. B.; Miller, C. K.; Webb, L. E. *J. Am. Chem. Soc.* **1964**, *86*, 2342.

(18) Larsen, N. G.; Boyd, P. D. W.; Rodgers, S. J.; Wuenschell, G. E.; Koch, C. A.; Rasmussen, S.; Tate, J. R.; Erler, B. S.; Reed, C. A. *J. Am. Chem. Soc.* **1986**, *106*, 6950.

Table IV. Positional Parameters and B(eq) Values for $PtCuCl_2N_8O_2C_{56}H_{52}$

atom	x	y	z	B(eq), Å^2	atom	x	y	z	B(eq), Å^2
Pt1A	0.8077 (1)	0.78326 (7)	0.5974 (1)	3.8 (1)	C22A	0.081 (2)	0.723 (2)	0.252 (3)	6 (1)
Pt1B	0.3344 (1)	0.20635 (7)	0.2531 (1)	4.0 (1)	C22B	−0.183 (2)	0.417 (2)	0.494 (3)	4.0 (9)
Cu1A	0.0178 (2)	0.1155 (2)	0.0381 (3)	2.7 (2)	C23A	−0.052 (7)	0.314 (5)	−0.24 (1)	32 (6)
Cu1B	0.4174 (3)	0.3934 (2)	0.5697 (3)	2.9 (2)	C23B	0.118 (3)	0.566 (2)	0.440 (4)	8 (1)
Cl1A	0.7394 (7)	0.7445 (5)	0.4334 (8)	6.1 (6)	C24A	0.168 (2)	0.140 (1)	−0.253 (3)	3.3 (8)
Cl1B	0.3789 (7)	0.2844 (4)	0.3759 (9)	5.7 (6)	C24B	0.182 (2)	0.435 (2)	−0.255 (3)	6 (1)
Cl2A	0.8867 (6)	0.8216 (4)	0.7564 (9)	5.5 (6)	C25A	0.216 (3)	0.179 (2)	−0.184 (4)	7 (1)
Cl2B	0.2987 (7)	0.1290 (4)	0.1217 (8)	6.3 (7)	C25B	0.119 (3)	0.405 (2)	0.653 (4)	9 (1)
N1A	0.036 (2)	−0.188 (1)	0.020 (2)	3.2 (6)	C26A	0.739 (3)	0.966 (2)	1.141 (4)	6 (1)
N1B	0.342 (1)	0.458 (1)	0.505 (2)	1.8 (5)	C26B	0.719 (2)	0.675 (2)	0.156 (3)	5 (1)
N2A	0.086 (1)	0.094 (1)	−0.059 (2)	2.0 (5)	C27A	0.185 (2)	−0.113 (1)	0.108 (3)	3.3 (8)
N2B	0.356 (1)	0.392 (1)	−0.331 (2)	1.7 (5)	C27B	0.598 (2)	0.227 (2)	0.847 (3)	4.5 (9)
N3A	0.935 (1)	0.961 (1)	0.906 (2)	2.4 (6)	C28A	0.087 (2)	−0.066 (2)	0.273 (3)	5 (1)
N3B	0.494 (2)	0.334 (1)	−0.358 (2)	3 (1)	C28B	0.683 (3)	0.233 (2)	0.689 (3)	6 (1)
N4A	−0.046 (1)	0.140 (1)	0.141 (2)	1.5 (5)	C29A	0.136 (2)	−0.052 (2)	0.382 (3)	6 (1)
N4B	0.478 (2)	0.390 (1)	0.471 (2)	4 (2)	C29B	0.678 (3)	0.183 (2)	0.611 (4)	10 (2)
N5A	0.708 (1)	0.001 (1)	−0.176 (2)	3.4 (6)	C30A	−0.075 (2)	0.130 (2)	0.408 (3)	5 (1)
N5B	0.425 (2)	0.192 (1)	−0.303 (2)	4 (2)	C30B	0.640 (2)	0.333 (2)	0.354 (3)	6 (1)
N6A	0.082 (2)	0.660 (1)	−0.212 (2)	5 (2)	C31A	−0.007 (3)	0.134 (2)	0.497 (4)	7 (1)
N6B	0.300 (2)	0.424 (1)	0.154 (2)	3.6 (6)	C31B	0.633 (3)	0.275 (2)	0.294 (4)	12 (2)
N7A	0.239 (1)	0.133 (1)	0.423 (2)	3.1 (6)	C32A	1.147 (2)	0.750 (2)	0.672 (3)	6 (1)
N7B	0.593 (2)	−0.155 (1)	−0.350 (3)	5.7 (8)	C32B	0.522 (2)	0.422 (2)	0.216 (3)	6 (1)
N8A	0.148 (2)	0.298 (1)	0.380 (2)	3.3 (6)	C33A	0.228 (2)	−0.040 (1)	−0.007 (2)	1.8 (6)
N8B	0.256 (2)	0.259 (1)	0.158 (2)	4.2 (8)	C33B	0.437 (2)	0.275 (1)	0.850 (3)	3.2 (8)
O1A	0.347 (1)	−0.060 (1)	0.305 (2)	6 (1)	C34A	0.296 (2)	−0.042 (1)	0.082 (2)	2.2 (6)
O1B	0.531 (2)	−0.092 (1)	0.298 (2)	6 (2)	C34B	0.431 (2)	0.217 (1)	−0.191 (3)	3.5 (7)
O2A	1.076 (2)	0.566 (1)	0.705 (3)	9 (2)	C35A	0.641 (2)	0.083 (2)	−0.075 (3)	5 (1)
O2B	0.193 (2)	0.442 (1)	0.029 (2)	6 (2)	C35B	0.574 (2)	0.821 (2)	0.115 (3)	5 (1)
C1A	0.095 (2)	0.768 (2)	−0.005 (3)	5.1 (9)	C36A	0.643 (2)	1.125 (1)	1.021 (3)	4.0 (8)
C1B	0.337 (2)	0.486 (1)	0.416 (3)	3.0 (7)	C36B	0.437 (2)	0.207 (2)	0.993 (3)	6 (1)
C2A	−0.123 (2)	0.273 (1)	−0.080 (3)	4 (2)	C37A	0.294 (2)	−0.127 (1)	−0.107 (3)	3.6 (7)
C2B	0.279 (2)	0.535 (2)	0.410 (3)	5 (1)	C37B	0.444 (2)	0.260 (2)	0.035 (3)	4.0 (8)
C3A	−0.078 (2)	0.258 (1)	−0.143 (3)	2.9 (7)	C38A	0.231 (2)	−0.085 (1)	−0.100 (3)	3.8 (8)
C3B	0.244 (2)	0.541 (1)	0.481 (3)	3.3 (7)	C38B	0.444 (2)	0.301 (2)	0.962 (3)	4.6 (9)
C4A	0.022 (2)	−0.202 (2)	0.113 (3)	5 (1)	C39A	1.174 (2)	0.714 (2)	0.881 (3)	3.8 (8)
C4B	0.283 (2)	0.491 (1)	0.538 (3)	3.7 (8)	C39B	0.376 (2)	0.495 (1)	0.255 (3)	3.3 (8)
C5A	0.960 (2)	0.828 (1)	1.159 (3)	3.1 (7)	C40A	−0.156 (2)	0.338 (2)	0.173 (3)	4.2 (8)
C5B	0.261 (2)	0.475 (1)	−0.379 (3)	3.0 (7)	C40B	0.330 (2)	0.475 (2)	0.159 (3)	5 (1)
C6A	0.906 (2)	0.871 (1)	1.125 (3)	3.3 (8)	C41A	0.792 (2)	0.386 (1)	0.192 (3)	3.8 (8)
C6B	0.294 (2)	0.427 (2)	0.674 (3)	4.3 (8)	C41B	0.319 (2)	0.499 (2)	0.062 (3)	7 (1)
C7A	0.849 (2)	0.894 (2)	1.175 (3)	4 (2)	C42A	1.282 (2)	0.623 (2)	0.844 (3)	5 (1)
C7B	0.254 (2)	0.408 (1)	−0.260 (3)	4 (2)	C42B	0.361 (3)	0.545 (2)	0.079 (4)	7 (1)
C8A	0.809 (2)	0.937 (2)	1.125 (3)	3.7 (8)	C43A	0.300 (2)	0.675 (2)	−0.102 (3)	4.4 (8)
C8B	0.309 (2)	0.363 (2)	0.777 (3)	3 (1)	C43B	0.405 (3)	0.567 (2)	0.174 (4)	6 (1)
C9A	0.145 (2)	0.053 (1)	−0.058 (3)	2.6 (8)	C44A	0.755 (2)	0.282 (2)	0.085 (3)	4.8 (9)
C9B	0.630 (2)	0.647 (1)	0.260 (2)	2.7 (7)	C44B	0.421 (2)	0.541 (2)	0.267 (3)	4.0 (9)
C10A	0.163 (2)	0.002 (1)	−0.001 (2)	2.9 (7)	C45A	0.316 (2)	−0.013 (1)	0.284 (3)	3.2 (7)
C10B	0.437 (2)	0.314 (2)	0.771 (3)	3.4 (9)	C45B	0.551 (2)	−0.137 (2)	0.348 (3)	3.6 (8)
C11A	0.885 (2)	1.003 (1)	0.932 (2)	2.7 (6)	C46A	0.708 (2)	−0.036 (1)	−0.366 (2)	2.2 (6)
C11B	0.494 (2)	0.303 (2)	−0.271 (3)	3.6 (8)	C46B	0.547 (2)	−0.127 (2)	0.465 (3)	3.8 (8)
C12A	0.868 (2)	1.055 (1)	0.876 (3)	3.3 (8)	C47A	0.744 (2)	−0.091 (1)	−0.350 (2)	2.6 (7)
C12B	0.565 (2)	0.263 (2)	0.754 (3)	5 (1)	C47B	0.408 (2)	0.164 (1)	0.456 (3)	4.0 (8)
C13A	−0.089 (2)	0.038 (1)	−0.188 (3)	2.3 (7)	C48A	0.256 (2)	0.120 (1)	0.529 (3)	4.0 (8)
C13B	0.388 (2)	0.735 (2)	0.305 (3)	5 (2)	C48B	0.444 (2)	0.104 (2)	0.318 (3)	6 (1)
C14A	0.047 (2)	0.020 (1)	0.177 (2)	1.9 (7)	C49A	0.709 (2)	0.937 (2)	0.449 (3)	4.1 (8)
C14B	0.560 (2)	0.310 (2)	0.627 (3)	5 (1)	C49B	0.492 (2)	0.063 (2)	0.383 (4)	6 (1)
C15A	0.001 (2)	−0.054 (1)	−0.231 (3)	3.2 (8)	C50A	0.691 (2)	−0.023 (1)	0.530 (3)	4.0 (8)
C15B	0.418 (2)	0.678 (2)	0.461 (3)	4 (2)	C50B	0.495 (2)	0.077 (2)	0.492 (4)	7 (1)
C16A	0.039 (2)	−0.111 (2)	−0.224 (3)	3.7 (8)	C51A	1.042 (2)	0.617 (2)	0.727 (3)	4.0 (8)
C16B	0.541 (2)	0.359 (2)	0.466 (3)	3.7 (9)	C51B	0.237 (2)	0.413 (2)	0.090 (3)	3.5 (8)
C17A	1.078 (2)	0.852 (1)	0.703 (3)	4 (2)	C52A	−0.045 (2)	0.633 (2)	−0.312 (3)	5 (1)
C17B	0.569 (2)	0.361 (2)	0.374 (3)	4 (1)	C52B	0.782 (2)	0.648 (1)	−0.094 (3)	3.0 (7)
C18A	0.111 (2)	−0.200 (2)	−0.266 (3)	4 (2)	C53A	−0.079 (3)	0.693 (2)	−0.338 (3)	6 (1)
C18B	0.482 (2)	0.595 (2)	−0.325 (3)	4.3 (9)	C53B	0.274 (2)	0.315 (2)	0.155 (3)	6 (1)
C19A	0.092 (1)	−0.192 (1)	−0.162 (2)	1.6 (5)	C54A	−0.187 (2)	0.659 (2)	−0.380 (3)	4.2 (9)
C19B	0.456 (2)	0.424 (1)	0.383 (3)	3.6 (8)	C54B	0.193 (3)	0.256 (2)	0.115 (3)	5 (1)
C20A	−0.121 (2)	0.237 (1)	0.097 (3)	3.5 (7)	C55A	0.161 (2)	0.395 (2)	0.357 (3)	6 (1)
C20B	0.607 (2)	0.532 (1)	−0.363 (3)	3.6 (8)	C55B	0.133 (2)	0.289 (2)	0.062 (3)	5 (1)
C21A	−0.183 (2)	0.325 (2)	−0.086 (3)	5.1 (9)	C56A	0.913 (2)	0.587 (2)	0.681 (3)	5 (1)
C21B	0.254 (2)	0.575 (2)	0.327 (3)	7 (1)	C56B	−0.151 (2)	0.657 (2)	−0.054 (3)	6 (1)

fragment in molecule B shows a similar but slightly smaller S_4 distortion. For example, the average dihedral angle between the mean planes of adjacent pyrrole rings of molecule B is 10.4°. In both molecules, the copper atom is essentially in the mean plane defined by the four pyrrole nitrogens with an out of plane displacement of less than 0.01 Å. The Cu–N distances range from 1.95 (3) to 2.02 (2) Å and are typical for copper porphyrins.

In accord with the far-IR analysis, the platinum fragments have trans geometries. The platinum atoms have a typical square-planar coordination with mean Pt–N distances of 1.99 (3) Å. These are similar to the Pt–N distances in *trans*-$PtCl_2(NC_5H_5)_2$.[19] The Pt–Cl distances range from 2.24 (1) to 2.29 (1) Å and are also

Table V. Selected Intramolecular Distances (Å) and Angles (deg) Involving the Non-Hydrogen Atoms for [Cu(DPE)]-$(py)_2PtCl_2$[a]

Distances			
Metal Coordination Spheres			
Pt1A–Cl1A	2.24 (1)	Cu1A–N3A	2.02 (2)
Pt1A–Cl2A	2.29 (1)	Cu1A–N4A	2.00 (2)
Pt1A–N7A	2.02 (2)	Cu1B–N1B	2.00 (2)
Pt1A–N8A	1.96 (3)	Cu1B–N2B	2.02 (2)
Pt1B–Cl1B	2.29 (1)	Cu1B–N3B	1.95 (3)
Pt1B–Cl2B	2.27 (1)	Cu1B–N4B	1.97 (3)
Pt1B–N7B	1.96 (3)	Cu1A–Cl2A	3.02 (1)
Pt1B–N8B	2.00 (3)	Cu1B–Cl1B	3.21 (1)
Cu1A–N1A	1.96 (3)	Pt1A–Pt1B	3.766 (3)
Cu1A–N2A	2.01 (2)		
Porphyrin Skeleton			
N1A–C1A	1.43 (4)	C2B–C21B	1.48 (5)
N1A–C4A	1.45 (4)	C3A–C4A	1.55 (5)
N1B–C1B	1.42 (3)	C3A–C22A	1.56 (5)
N1B–C4B	1.34 (4)	C3B–C4B	1.48 (4)
C1A–C2A	1.53 (4)	C3B–C22B	1.41 (4)
C1A–C20A	1.41 (4)	C4A–C5A	1.47 (5)
C1B–C2B	1.41 (4)	C4B–C5B	1.44 (4)
C1B–C20B	1.40 (4)	C5A–C6A	1.32 (4)
C2A–C3A	1.31 (4)	C5B–C6B	1.37 (4)
C2A–C21A	1.49 (5)	C22A–C23A	1.1 (1)
C2B–C3B	1.27 (4)	C22B–C23B	1.36 (5)
Nicotinoyl Groups			
N5A–C34A	1.38 (3)	C45A–C46A	1.48 (4)
N5A–C45A	1.41 (4)	C45B–C46B	1.50 (4)
N5B–C34B	1.42 (4)	C46A–C47A	1.34 (4)
N5B–C45B	1.33 (4)	C46A–C50A	1.38 (4)
N6A–C40A	1.38 (4)	C46B–C47B	1.44 (4)
N6A–C51A	1.37 (4)	C46B–C50B	1.38 (5)
N6B–C40B	1.45 (4)	C48A–C49A	1.42 (4)
N6B–C51B	1.28 (4)	C48B–C49B	1.40 (5)
N7A–C47A	1.28 (3)	C49A–C50A	1.33 (4)
N7A–C48A	1.39 (4)	C49B–C50B	1.37 (5)
N7B–C47B	1.35 (4)	C51A–C52A	1.57 (5)
N7B–C48B	1.30 (4)	C51B–C52B	1.59 (4)
N8A–C53A	1.26 (4)	C52A–C53A	1.50 (5)
N8A–C54A	1.42 (4)	C52A–C56A	1.46 (5)
N8B–C53B	1.46 (4)	C52B–C53B	1.38 (4)
N8B–C54B	1.18 (4)	C52B–C56B	1.29 (5)
O1A–C45A	1.18 (3)	C54A–C55A	1.32 (5)
O1B–C45B	1.30 (4)	C54B–C55B	1.31 (5)
O2A–C51A	1.25 (4)	C55A–C56A	1.36 (5)
O2B–C51B	1.19 (4)	C55B–C56B	1.46 (5)
Angles			
Metal Coordination Spheres			
Cl1A–Pt1A–Cl2A	174.2 (4)	N1A–Cu1A–N2A	95 (1)
Cl1A–Pt1A–N7A	93.5 (8)	N1A–Cu1A–N3A	175 (1)
Cl1A–Pt1A–N8A	86.8 (8)	N1A–Cu1A–N4A	85 (1)
Cl2A–Pt1A–N7A	87.3 (8)	N2A–Cu1A–N3A	88 (1)
Cl2A–Pt1A–N8A	92.4 (8)	N2A–Cu1A–N4A	176 (1)
N7A–Pt1A–N8A	179 (1)	N3A–Cu1A–N4A	93 (1)
Cl1B–Pt1B–Cl2B	174.1 (4)	N1B–Cu1B–N2B	90 (1)
Cl1B–Pt1B–N7B	87 (1)	N1B–Cu1B–N3B	176 (1)
Cl1B–Pt1B–N8B	92.5 (9)	N1B–Cu1B–N4B	92 (1)
Cl2B–Pt1B–N7B	93 (1)	N2B–Cu1B–N3B	89 (1)
Cl2B–Pt1B–N8B	87.5 (9)	N2B–Cu1B–N4B	177 (1)
N7B–Pt1B–N8B	177 (1)	N3B–Cu1B–N4B	89 (1)

[a] Estimated standard deviations in the least significant figure are given in parentheses.

very similar to those reported in the literature.[19]

An unusual structure feature of the binuclear Cu–Pt complexes is the nearly perpendicular orientation of the CuN_4 and $PtCl_2N_2$ planes. In molecule A, the dihedral angle formed by these two planes is 75°. The corresponding dihedral angle in molecule B is 83°. This points a Cl directly at the Cu. In molecule B, the Cu–Cl distance is 3.21 (1) Å. However, in molecule A, the Cu–Cl distance is much shorter (3.02 (1) Å). In other square-pyramidal copper(II) complexes in which a chlorine ligand from an adjacent metal fragment serves as the apical ligand on Cu, the Cu–Cl distances range from 2.41 to 3.36 Å.[20] Although it is clear that Cu interacts with a platinum-bound chloride, the Pt–Cl distances are not significantly perturbed by this interaction.

The most surprising aspect of the structural analysis is the short Pt_A–Pt_B distance (3.766 (3) Å) within the asymmetric unit. In *trans*-$PtCl_2(NC_5H_5)_2$, the shortest Pt–Pt distance is 5.542 Å. In $Pt(NH_3)_2Cl_2$ and $Pt(en)Cl_2$, Pt–Pt distances are approximately 3.40 Å. The typical Pt–Pt distances in columnar Pt(II) complexes are 3.09–3.75 Å.[21] Thus, a weak Pt–Pt interaction is likely to exist between molecules A and B.

Concluding Remarks

Attachment of two nicotinoyl appendages to the same face of α,α-bis(*o*-aminophenyl)etioporphyrin produces a ligand system with two unique metal binding sites. The methyl groups flanking the *o*-aminophenyl substituents provide sufficient steric hinderance to minimize atropisomerization and loss of the chelating ability of the bis(pyridine) site. Thus, it is possible to prepare binuclear complexes in a preconceived manner by first metalating the porphyrin and subsequently adding a second metal. This versatility allows for a high degree of chemical control. Using this approach, we have prepared several new dinuclear metal complexes.

The single-crystal X-ray analysis of [Cu(DPE)]-$(py)_2PtCl_2$ is one of the few examples in which a "tailed" porphyrin has been structurally characterized.[18,22] Of conceptual interest are two potentially important aspects of our dinuclear complexes. Because it should be possible to design the coordination sphere of metals in the pyridine binding site to contain labile ancillary ligands, it may be possible to generate a vacant coordination site for metal-mediated reactions. In addition, the ability of both metals to interact with the same ligand simultaneously may lead to new modes of molecular activation or recognition.

Acknowledgment. Financial support of this work was provided by the DOE, Contract W-7405-Eng-82, administered by the Ames Laboratory.

Supplementary Material Available: Text detailing the data collection and listings of atomic coordinates, thermal parameters, bond distances and angles, and least-squares planes for **2** and **5** (79 pages); listings of calculated and observed structure factors for **2** and **5** (90 pages). Ordering information is given on any current masthead page.

(19) Colamarino, P.; Orioli, P. L. *J. Chem. Soc., Dalton Trans.* **1975**, 1656.

(20) (a) Baker, R. J.; Nyburg, S. C.; Szymanski, J. T. *Inorg. Chem.* **1971**, *10*, 138. (b) Harker, D. *Z. Kristallogr.* **1936**, *93*, 136. (c) Marsh, W. E.; Hatfield, W. E.; Hodgson, D. J. *Inorg. Chem.* **1982**, *21*, 2679. (d) Willett, R. D.; Chang, K. *Inorg. Chim. Acta* **1970**, *4*, 447. (e) O'Bannon, G.; Willett, R. D. *Inorg. Chim. Acta* **1981**, *53*, L131. (f) Wells, A. F. *J. Chem. Soc.* **1947**, 1670. (g) Gunter, M. J.; Mander, L. N.; McLaughlin, G. M.; Murray, K. S.; Berry, K. J.; Clark, P. E.; Buckingham, D. A. *J. Am. Chem. Soc.* **1980**, *102*, 1470.

(21) (a) Gliemann, G.; Yersin, H. *Struct. Bonding* **1985**, *62*, 87. (b) Williams, J. M. *Adv. Inorg. Chem. Radiochem.* **1983**, *26*, 235. (c) Krogmann, K. *Angew. Chem., Int. Ed. Engl.* **1969**, *8*, 35.

(22) (a) Bobrik, J. A.; Walker, F. A. *Inorg. Chem.* **1980**, *19*, 3383. (b) Mashiko, T.; Reed, C. A.; Haller, K. J.; Kastner, M. E.; Scheidt, W. R. *J. Am. Chem. Soc.* **1981**, *103*, 5758.